Applied Catalysis A: General 529 (2017) 32–39

Contents lists available at ScienceDirect

Applied Catalysis A: General

journal homepage: www.elsevier.com/locate/apcata

Metal-surfactant interaction as a tool to control the catalytic selectivity of Pd catalysts

A.M. Perez-Coronado[a], L. Calvo[a,*], J.A. Baeza[a], J. Palomar[a], L. Lefferts[b], J.J. Rodriguez[a], M.A. Gilarranz[a]

[a] Sección Departamental de Ingeniería Química, C/Francisco Tomás y Valiente 7, Universidad Autónoma de Madrid, 28049, Madrid, Spain
[b] Catalytic Processes and Materials, MESA+ Institute for Nanotechnology, University of Twente, Enschede 7500AE, The Netherlands, The Netherlands

ARTICLE INFO

Article history:
Received 4 July 2016
Received in revised form 7 October 2016
Accepted 15 October 2016
Available online 17 October 2016

Keywords:
Palladium
Nanoparticles
Catalysis
AOT
Nitrite

ABSTRACT

The catalytic activity of Palladium nanoparticles synthesized via sodium bis[2-ethylhexyl] sulfosuccinate (AOT)/isooctane reverse microemulsion was studied in nitrite reduction. The influence of reaction conditions and the synthesis and purification of the nanoparticles was evaluated. In the nanoparticle size range studied (6.2–11.6 nm) a lower reaction rate and TOF were observed for small nanoparticles. This apparent structure sensitiveness results from surface blockage due to interaction of AOT with the surface of nanoparticles, as evidenced by purification with several solvents providing different removal of AOT. The activity loss was accompanied by negligible selectivity to ammonium. Large nanoparticles in buffered medium produced insignificant amount of ammonium ion for nitrite conversion values of ca. 80%. The selectivity control is ascribed to preferential blockage of the sites responsible for ammonium generation. The results show the potential of the interaction between the AOT and the nanoparticles as a tool to control catalytic selectivity.

1. Introduction

Most of the metal-based catalysts prepared at industrial scale are commonly synthesized through few conventional steps [1]. These steps involve the impregnation/precipitation of a precursor of the active phase on a support, a calcination treatment and, finally, a reduction stage, e.g. in hydrogen. Catalysts with high activity, selectivity or stability can be achieved following this procedure, but no precise control of size and structure of the active phase can be achieved.

The preparation of rationally-designed catalysts with high performance is still one of the classical challenges in catalysis [2,3]. Since the performance of metallic catalysts is closely linked to the structure of the metal phase, the methods of control of nanoparticle (NP) size have gained important attention in the last years as a strategy to facilitate rational design [4–7], particularly in the case of structure sensitive reactions. Chemical methods have been proved to be especially interesting due to their effectiveness and simplicity [8]. These methods have in common the use of a reducing agent, which reduces the metal precursor to metal NPs, in presence of stabilizing agent (SA) limiting the NPs growth and preventing their aggregation. SAs are also named as capping agents, surfactants or ligands in the literature. Many different organic compounds have been successfully used as SA, such as polyvinylpyrrolidone (PVP), polyvinyl alcohol (PVA), sodium bis[2-ethylhexyl] sulfosuccinate (AOT), cetyltrimethylammonium bromide (CTAB), ascorbic acid (AA) and polyethylene glycol (PEG), among others [6]. The SA remaining in the synthesis medium or on the NPs surface after the catalysts synthesis has been considered as a drawback, since they usually interact strongly with the metallic phase/support and can have an impact the catalyst performance [9]. Thus, the metal surface can be hindered making them less accessible to the reactants, or the active centres can be blocked by the groups of the SA attached to metal surface. Different approaches have been used to remove SAs and promote activity. The most common procedure is washing of NPs after synthesis with solvents of different polarity, which is quite efficient in the removal of the excess of SA, but does not remove it completely [10]. Decomposition of SA through thermal or oxidizing treatments [11] achieves removal of SAs, but some side problems such as sintering, deposition of coke on the metal surface or partial oxidation of the NPs can occur. The weakening of bonds between the SA and the metal surface through competition with chemicals exhibiting higher affinity for the SA or metal surface has also been described [2].

* Corresponding author.
E-mail address: luisa.calvo@uam.es (L. Calvo).

http://dx.doi.org/10.1016/j.apcata.2016.10.013
0926-860X/

Although the removal of SA after washing NPs is an important concern, some authors have reported that the lower catalytic activity provoked by the presence of the SA was accompanied by changes in selectivity [12–15]. The diasteroselective hydrogenation of cinchonide, the hydrogenation of citral or phenylacetone, and the isomerization of ally alcohols to carbonyl compounds, catalysed by noble metal-based catalysts, are among the reactions in which this phenomenon was observed. The research on this issue is still scarce, but Niu and Li [2] have differentiated different mechanism through which SAs can modify selectivity. The role of the SA in the promotion of selectivity has especial interest in those cases where the interaction between SA and metal surface is strong enough to result in stable performance of the catalyst. Thus SAs can become a tool for rational design of high-performance catalysts. Further research is still needed in this promising field to address questions such as how the SA is attached to the NPs surface, what is the surface coverage, what is the interaction between reactant and the SA or how is the charge transfer between SA and metal surface, among others.

The surfactant agents used for the preparation of NPs by microemulsion (ME) methods exhibit a particularly strong interaction with the metallic active phase of the catalysts due to their amphipilic character and functional groups. Amphiphiles can be cationic (e.g CTAB, benzalkonium chloride (BZC)), anionic (e.g AOT, sodium dodecyl benzene sulfonate (SDBS), lauryl sodium sulfate (SDS)) or non-ionic (e.g Triton X-100, polyoxyethylated lauryl ether (Brij 30)) depending on the nature of their head groups. Among these surfactants, AOT is one of the most used in the synthesis of metallic, metal sulfide and metal oxide NPs in water/oil suspension, since the use of a co-surfactant to lower the microemulsion surface tension can be avoided [16].

The NPs resulting from synthesis in AOT-based ME systems have high stability, small particle size, and good monodispersity. Due to its higher solubility in organic phase, AOT helps to extract metal cations from the aqueous to reverse micellar phase. In addition the NPs formed in AOT-based ME have relatively strong electrostatic interactions with the negatively charged head polar group of AOT molecules, which provides with a protective effect against aggregation. However, the NPs may suffer from blocking due to interaction with AOT, which leads to lower values of available catalyst surface area. Sato et al. [17] prepared Pd NPs in reverse micelles using KBH_4 as reducing agent and showed that their hydrogenation activity was inhibited by the AOT remaining on the surface NPs. The difficulty to removed AOT from metal surface has been attributed to the presence of sodium and sulphur [18]. Thus, AOT removal from NPs surface has been considered necessary to minimize the blocking of active centres. However literature works on the interaction between AOT and metal NPs are scarce [19]. Specifically, to the best of our knowledge, there are no works dealing in depth with the interaction between AOT and Pd surface.

The aim of this work is to study the control of the catalytic activity and selectivity for Pd NPs synthesized in the AOT/isooctane reverse (water in oil) ME system, using the reduction of nitrite as a model reaction. Also, the influence of the pH conditions on the activity and selectivity of the nitrite reduction process was emphasized. The influence of the conditions for the synthesis and purification of the Pd NPs are evaluated.

2. Experimental

2.1. Materials

Tetraammine palladium (II) chloride monohydrate ($Pd(NH_3)_4Cl_2{\cdot}H_2O$) (≥99%, Sigma-Aldrich Co.) was used as palladium precursor, isooctane (99.8%, Sigma-Aldrich Co.) as oil phase, and hydrazine hydrate solution (50–60%, Fluka) as reducer. The Dioctyl sulfosuccinate sodium salt (AOT; 98%, Sigma) used as surfactant was vacuum-dried for 24 h at 333 K before use. Sodium nitrite (≥99%, Panreac) was used to prepare nitrite solutions for the catalytic activity experiments. Demineralized bidistilled water was used throughout this work (Nihon Millipore Ltd.).

2.2. Synthesis and characterization of Pd NPs in microemulsion nanoparticles

The preparation of Pd NPs was carried out through the reduction of $Pd(NH_3)_4Cl_2{\cdot}H_2O$ with hydrazine in AOT/isooctane reverse (water in oil) micellar solution. The reduction was achieved by mixing equal volumes of two reverse micellar solutions prepared with w_0 (water to AOT molar ratio) values of 3, 7 and 12, and an AOT concentration of 0.35 M in isooctane. After a 10 min of reduction, isooctane was evaporated in a rotary evaporator at 368 K and the NPs were purified from excess of surfactant by addition of solvent followed by centrifugation (this washing was carried out three times). The solvents considered for purification were methanol (MeOH), tetrahydrofuran (THF) and tri-fluoroethanol (TFE). The Pd NPs synthesized were characterized by transmission electron microscopy (TEM) at 200 kV (JEOL, mod. JEM-2100). Samples were prepared placing a drop of microemulsion Pd NPs onto a carbon-coated copper grid and letting it dry at room temperature. Software 'ImageJ 1.44i' was used for counting and measuring particles on digital TEM images (more than 200 NPs were measured per sample using different images for that). Surface-area-weighted mean diameters, Eq. (1), and size distribution, characterized by the standard deviation, Eq. (2), were calculated as described elsewhere [20].

$$d_s = \frac{\sum n_i \cdot d_i^3}{\sum n_i \cdot d_i^2} \quad (1)$$

$$\sigma_s = \sqrt{\frac{\sum (d_i - d_s)^2}{n}} \quad (2)$$

The specific surface area of Pd NPs was calculated assuming spherical shape from Eq. (3).

$$SSA_{Pd} = \frac{6}{d_s \cdot \rho_{Pd}} \quad (3)$$

Likewise, the catalysts were characterized by (XPS) (Physical Electronics, mod. K-Alpha equipped with a Al-Kα X-ray excitation source, 1486.68 eV). Samples for XPS analysis were evaporated on an aluminium grid under nitrogen atmosphere at ambient temperature to avoid oxidation. Software "Multipak v8.2b" was used for deconvolution in order to determine both Pd electrodeficient and zerovalent species in the particle surface. C 1 s peak (284.6 eV) was used as internal standard for binding energies [21]. Deconvoluted peaks showed binding energies in the range of 334.8–335.8 eV and 336.2–337.1 eV for Pd 3d5/2 which can be attributed to metallic Pd (Pd^0) and electron-deficient Pd (Pd^{n+}), respectively. All this data values are in good agreement with those reported at NIST X-ray Photoelectron Spectroscopy Database [21]. A probing depth of several nanometres can be assumed.

2.3. Nitrite reduction experiments

Nitrite reduction experiments were carried out during 4 h in a jacketed glass batch reactor where H_2 was continuously fed at 50 cm^3(STP) min^{-1} flow rate under vigorous stirring (500–700 rpm) in order to facilitate hydrogen distribution through the nitrite solution (150 mL and 50 mg NO_2^-/L). Former works using this set-up showed that the system is not subjected to constrain due to hydrogen transfer or external diffusion [22,23]. The reaction temperature (303 K) was controlled by a thermostatic

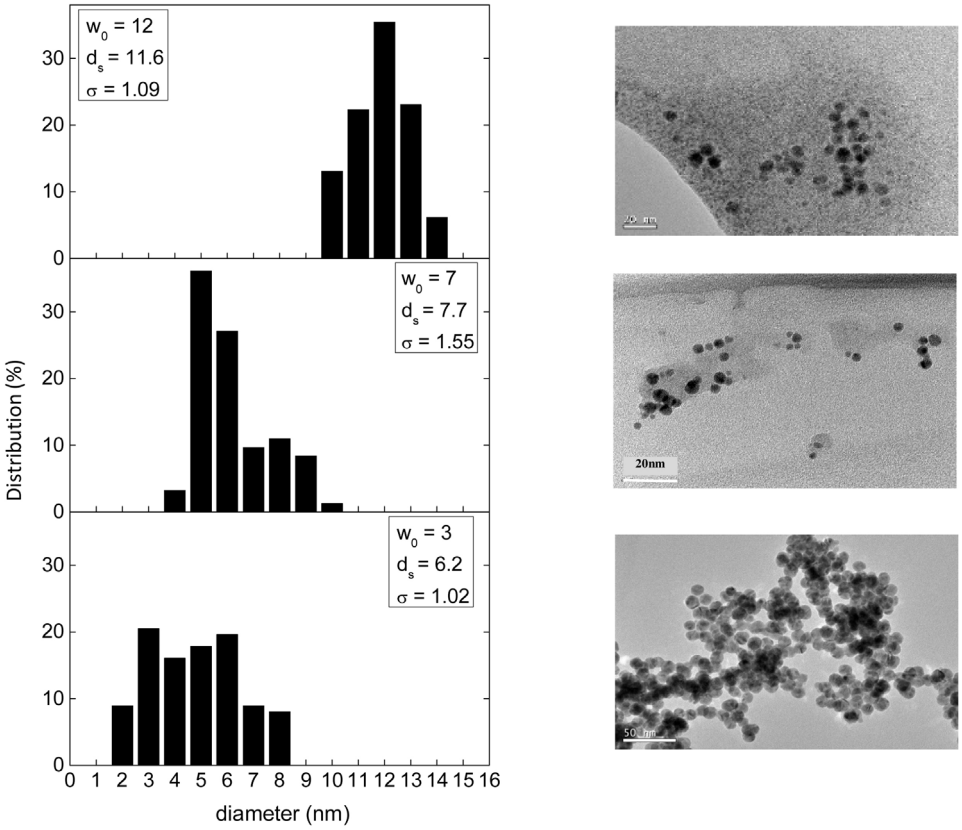

Fig. 1. Particle size distribution and TEM images of the NPs samples obtained at different water-to-surfactant molar ratios.

bath connected to the reactor jacket. In some experiments the pH of the reaction medium was buffered at a pH value around 6. Pure carbon dioxide was bubbled (50 cm^3(STP) min^{-1}) for 30 min through 140 mL of water containing the Pd NPs suspension under vigorous stirring. Then, 10 mL of a 750 mg/L NO_2^- solution was added and H_2 was fed (50 cm^3(STP) min^{-1}) together with carbon dioxide. 1 mL samples were withdrawn from the reactor at 0, 5, 15, 30 and 60 min until the end of the reaction experiment. The samples were filtered over 0.22 μm pore size PTFE filters and analyzed by ion chromatography (Metrohm 790 Compact IC Plus) using a Metrosep C4 column and a mixture of 1.7 mM HNO_3 and 0.7 mM 2,6-pyridinedicarboxylic acid as mobile phase to analyze the ammonium concentration. To analyze nitrite concentration a MetrosepASupp 5 column and a mixture of mM NaHCO 3.20 and 1.00 mM Na_2CO_3 were used. A simple pseudo-first order kinetic equation was used to describe the rate of nitrite disappearance. Since hydrogen is used in excess, its concentration was included into the pseudo-first-order rate constant ($k_{nitrite}$):

$$(-\mathbf{r}) = \frac{-\mathbf{dC_{nitrite}}}{\mathbf{d}t} = \mathbf{k_{nitrite}} \cdot \mathbf{C_{nitrite}} \quad (4)$$

The catalytic activity was calculated from the pseudo-first-order constant according to Eq. (5),

$$\mathbf{a} = \mathbf{k_{nitrite}} \cdot \frac{\mathbf{C_{nitrite}}}{,} 0\mathbf{C_{Pd}} \quad (5)$$

The values of turnover frequency (TOF) were calculated in the case of reactions buffered with CO_2 [24]. This parameter provides the number of revolutions of the catalytic cycle per unit of time and per number of active sites, and it is calculated from the first-order rate constant as follows:

$$\mathbf{TOF}\left(\boldsymbol{min}^{-1}\right) = \frac{\mathbf{k_{nitrite}}}{.}\mathbf{c_{nitrite}} \cdot \mathbf{S_{Pd}} \cdot \mathbf{N_A SSA_{Pd}} \cdot \mathbf{M_{nitrite}} \quad (6)$$

where S_{Pd} is the surface occupied by one Pd-atom (0.0787 nm^2), N_A is the constant of Avogadro, SSA_{Pd} is the specific surface area of Pd avalilabe and $M_{nitrite}$ is the molar mass of nitrite. TOF was calculated assuming a pseudo-spherical shape of NPs and all surface sites were taken into account, thus ignoring any potential blocking of metal NPs by AOT.

The selectivity to ammonium was defined as:

$$\textbf{ammonium selectivity } (\%) = \frac{\textbf{mole of ammonium formed}}{\textbf{mole of nitrite converted}} \cdot \mathbf{100} \quad (7)$$

3. Results and discussion

3.1. Pd NPs size and size distribution

Pd NPs were prepared under different values of w_0 in order to obtain Pd NPs with different size and study the sensitiveness of the nitrite reduction reaction to structure of the NPs. Fig. 1 shows representative TEM images and the size distribution for the Pd NPs synthesized under the different conditions tested. The Pd NPs exhibited pseudo-spherical shape in the TEM images. Table 1 shows the average mean diameter (d_s) and the size distribution (σ_s) calculated from the histograms shown in Fig. 1. As a general trend, the mean NPs size increased with w_0, which was particularly evident for a w_0 value of 12. It has been reported that the role of AOT is to act as a protecting agent, allowing control of NPs growth during microemulsion synthesis. An increase of this ratio for a constant concentration of surfactant will increase the average diameter of the droplets and consequently the size of the NPs [26]. According to σ_s no significant differences were found in size distribution,

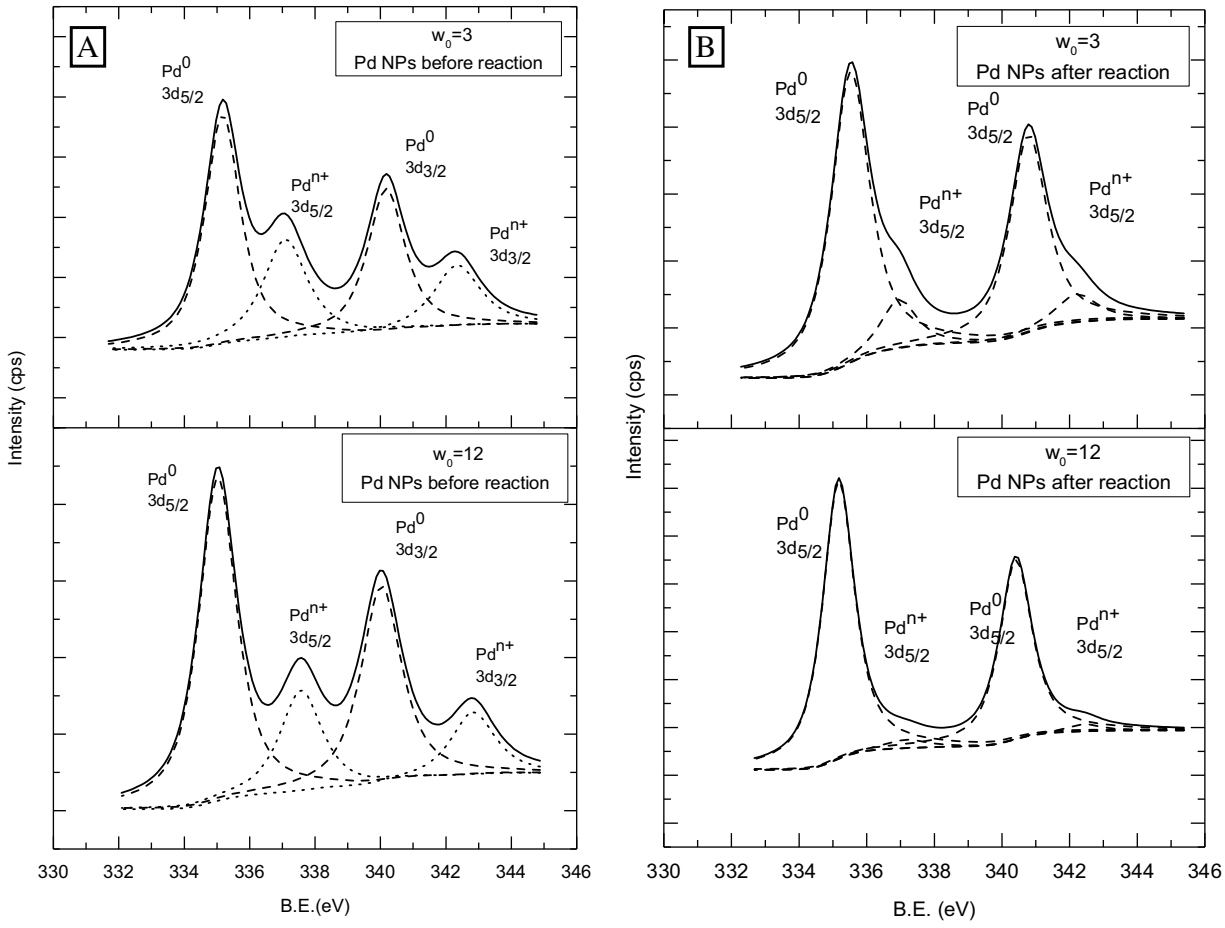

Fig. 2. XPS spectra of Pd NPs synthesized with w_0 values of 3 and 12 for: A) Pd NPs before reaction and B) Pd NPs after exposure in water to H_2 for 4 h at 303 K.

Table 1
Characterization of Pd NPs and kinetic parameters for the reduction or nitrite (NPs purified with MeOH, buffered medium, 2.45 mgPd/L).

w_o	d_s (nm)	SSA Pd (m^2/g_{Pd})	$k_{nitrite}$ (min^{-1})	R^2	Pd^{n+}/Pd^0 ratio before reaction	Pd^{n+}/Pd^0 ratio after reaction	a (mmol/g_{Pd} min)	TOF (min^{-1})
3	6.2	80.5	$4{\cdot}10^{-3}$	0.99	0.55	0.15	1.394	0.821
7	7.7	65.2	$7\ 10^{-3}$	0.99	n.m.	n.m	3.287	2.392
12	11.6	43.1	$15{\cdot}10^{-3}$	0.99	0.35	0.04	6.029	6.803

although a wider range of size was observed for the NP samples synthesized at lower w_0.

3.2. XPS characterization

XPS was used to establish the oxidation state of Pd. Fig. 2 shows the Pd 3d region deconvolved spectra for the NPs synthesized with $w_0 = 3$ and 12 before use in reaction (Fig. 2A) and after exposure in water to H_2 for 4 h at 303 K (Fig. 2B). As can be seen in Table 1 and Fig. 2A, the smallest particles (6.2 nm) show initial Pd^{n+}/Pd^0 ratios of 0.55, whereas for the largest particles (11.6 nm) that initial ratio is 0.35. The presence of both Pd^{n+} and Pd^0 was observed in Pd NPs series synthesized with w_0 of 3 and 12. These results are in good agreement with previous ones reported in the literature, where larger Pd NPs synthetized via microemulsion had a lower Pd^{n+}/Pd^0 ration than smaller ones [27]. Other authors also indicated that small particles are oxidized more easily thus leading to higher Pd^{n+}/Pd^0 ratios [22,28]. After exposure to H_2 in conditions equivalent to those of nitrite reduction reaction both the small and large NPs were reduced, since Pd^{n+}/Pd^0 ratios decreased to 0.15

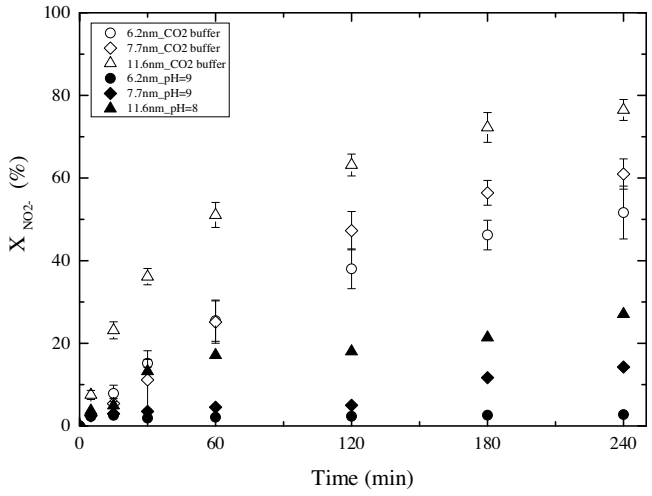

Fig. 3. Influence of Pd NPs size and pH of the reaction medium on nitrite conversion (NPs purified with MeOH, 2.45 mg Pd/L).

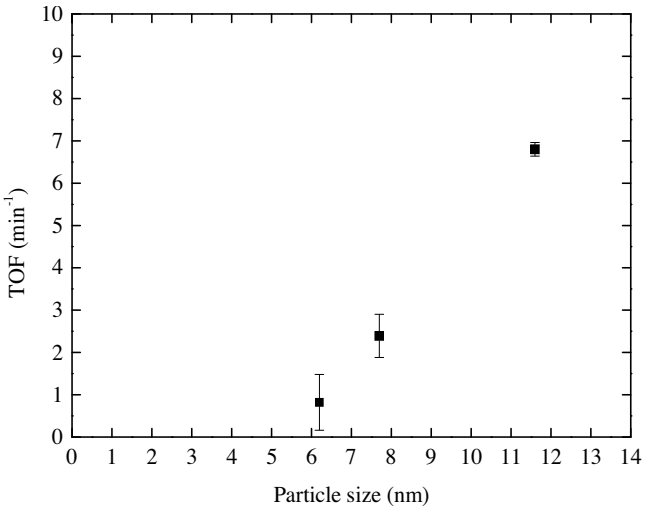

Fig. 4. TOF as function of NP size (purification with MeOH; reaction: buffered medium, 2.45 mg Pd/L).

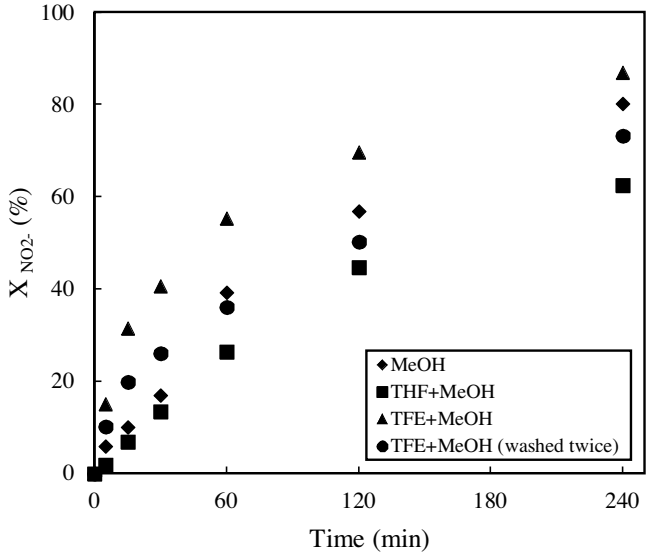

Fig. 5. Conversion of nitrite in runs with Pd NPs purified with different solvents (synthesis: $w_0 = 7$; dp = 7.7 nm; reaction: buffered medium, 7.7 mg Pd/L).

and 0.04 (Fig. 2B), respectively. Again higher Pd^{n+}/Pd^0 ratio was observed for the smallest NPs.

3.3. Nitrite reduction with unsupported Pd NPs

Fig. 3 shows the evolution of nitrite conversion upon reaction time with unsupported Pd NPs washed with methanol using a concentration of 2.45 mg Pd/L, for both buffered and non-buffered experiments. In these last experiments nitrite reduction was extremely slow and the final conversion varied between 5% (6.2 nm NPs) and 22% (11.6 nm NPs). The pH of the reaction medium varied between 8 and 9.3 due to the hydroxide ions from the nitrite reduction reaction. These results are in good agreement with other works, where low catalytic activity was ascribed to blockage of the palladium active sites by the OH^- ions generated during nitrite reduction [28–32]. Thus, the pH was found as a key parameter in nitrite conversion, since substantially higher values (50–80%) were achieved when the reaction medium was buffered with CO_2.

As can also be seen in Fig. 3, significant differences were found in nitrite conversion depending on the Pd NPs size. Larger sizes (higher w_0, less AOT) always led to higher nitrite conversion, regardless the pH of the reaction medium. These results show some discrepancies with most of the works in literature [23], where the nitrite reduction is described as a size-independent reaction. Our results show that the synthesis method and/or the AOT remaining on the surface of the NPs after washing with methanol influence their catalytic behaviour. Thus, activity and TOF increased with Pd NPs size (Table 1, Fig. 4), which was not expected from the common trend reported in other works and the much lower specific surface area of the larger NPs. Chinthaginjala et al. [33,34] reported that the TOF for Pd catalysts in nitrite reduction is independent of Pd NPs size in the range from 2.6 to 30 nm. Zhao et al. [23] observed that the TOF value for nitrite reduction using Pd-PVA colloids as catalyst is independent of particle size in the 2.2–20 nm range.

The trend shown by Fig. 4 suggests that i) the number of exposed Pd sites increases with the NPs size, which does not follow the general assumptions in TOF calculation; ii) the active sites on large NPs are more active, and/or iii) an apparent structure sensitiveness results from the interaction between AOT and the NPs. Larger NPs are expected to retain on their surface a lower amount of AOT even after purification, due to the higher w_0 used in the synthesis. Likewise, small size NPs can be expected to interact more strongly with anionic AOT species due to higher prevalence of both low coordination sites and electron-deficient species. As a result, lower removal of AOT would take place in the purification stage.

In a previous work [25], EDXS technique was employed to study the removal of AOT during the purification of the nanoparticles. The EDXS spectra showed that after three washing steps with methanol the intensity of the S peak corresponding to the sulfonate group of AOT decreased dramatically. The very low signal observed indicated that the amount to AOT on the surface of the nanoparticles was very low. TGA analysis of the purified nanoparticles after deposition on an activated carbon support (5% Pd/C, Norit SX PLUS, see Figure in Supplementary material) evidenced the low amount of AOT remaining in the nanoparticles after purification.

In spite of the low amount of AOT on the purified nanoparticles, important alteration of the catalytic behaviour was observed. Therefore, alternative purification of the NPs was carried out with solvents of increasing acidity: TFE > MeOH > THF. The lower acidity of THF results in a lower capability for the removal of AOT from the surface of the NPs, due to the weak electrostatic interaction between the solvent and anionic AOT species. As can be seen in Fig. 5, the NPs purified by washing with a THF + MeOH mixture are less active in the nitrite reduction for an identical particle size (7.7 nm). On the contrary, when NPs were purified with a solvent mixture with a higher acidity (TFE + MeOH), which results in higher AOT removal, a higher nitrite disappearance rate was obtained. After three washes with the TFE + MeOH mixture ca. 19% of the purified NPs could not be recovered by centrifugation and incorporated to the reaction medium. Interestingly, in this experiment much faster disappearance of nitrite was observed even though the metal concentration was slightly lower. These results are summarized in Table 2 and support the hypothesis that the interaction between AOT and the Pd NPs reduces the accessible surface area.

Additional reaction experiments were carried out at different metal concentration in the reaction medium (2.45, 7.7, and 23 mg Pd/L). The NPs selected were those synthesized with a water-to-surfactant ratio of 7 (7.7 nm) and purified with MeOH. Fig. 6 indicates a coherent increase in the conversion of nitrite at increasing concentration of Pd in the reaction medium, both for buffered and non-buffered reactions. Conversion values up to 92% were achieved within the reaction time considered for the highest Pd concentration. In the low metal concentration range (<10 mg Pd/L) the increase of the rate constant with catalyst concentration, and therefore the increase of hydrogen consumption, confirms that the

Table 2
Kinetic constant ($k_{nitrite}$), (SSA_{Pd}), activity (a) and TOF calculated for nitrite reduction using different solvents for the purification of NPs (synthesis: $w_0 = 7$; dp = 7.7 nm; reaction: buffered medium, 7.7 mg Pd/L).

Solvent	$k_{nitrite}$ (min^{-1})	R^2	a (mmol/g Pd min)	TOF (min^{-1})
MeOH	$7{\cdot}10^{-3}$	0.98	0.989	0.719
THF + MeOH	$4{\cdot}10^{-3}$	0.99	0.587	0.433
TFE + MeOH[b]	$8{\cdot}10^{-3}$	0.97	1.823	1.782
TFE + MeOH[a]	$5{\cdot}10^{-3}$	0.98	0.721	0.538

[a] Washed twice.
[b] 6.2 mgPd/L (19% Pd NPs lost during 3rd wash).

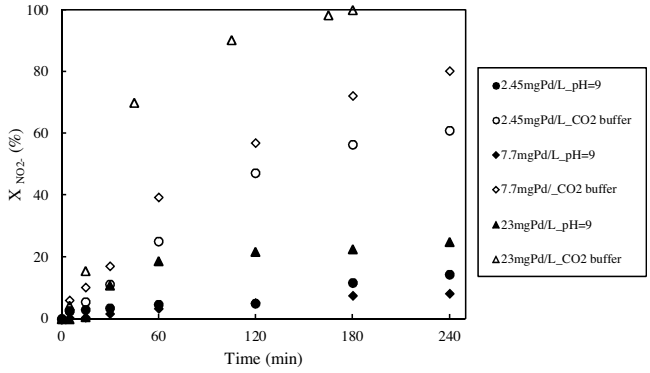

Fig. 6. Influence of Pd concentration and pH of the reaction medium in nitrite conversion (synthesis: $w_0 = 7$, $d_s = 7.7$ nm, NPs purified with MeOH).

reaction occurred under chemical control. The activity values normalized for Pd concentration and the TOF did not show significant changes when the metal load increased from 2.45 to 23 mg Pd/L (Table 3, Fig. 7).

Significant differences in selectivity were also observed depending on the NPs size and the pH of the reaction medium (Fig. 8). The influence of NPs size was more evident at high pH, where selectivity to ammonium was around 5% for the largest NPs and well above 30% for the smallest; on the contrary, very low selectivity towards ammonium was observed in the case of the reaction carried out in buffered medium. Thus, ammonium ion was in the detection limit for the largest NPs and at very low values below 0.08 mg/L for the smallest, with selectivity values below 1% in all cases. At any nitrite conversion value, the selectivity to ammonium was higher for smallest NPs, as can be seen in Fig. 8B. The selectivity to ammonium for the smallest NPs remained at low values up to 25% conversion and beyond that a substantial increase was observed.

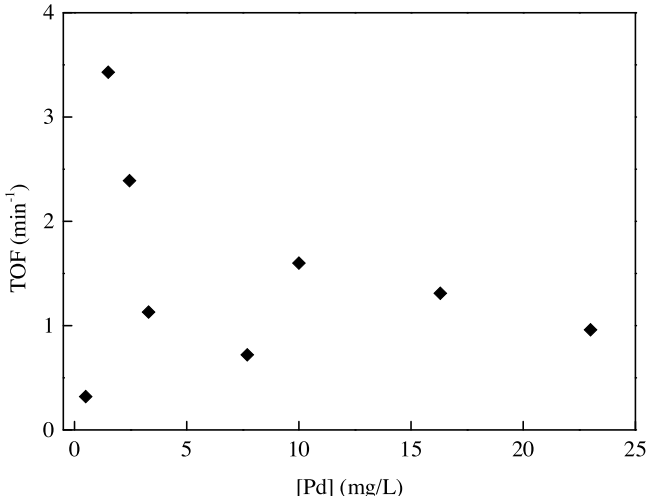

Fig. 7. TOF versus Pd NPs concentration (synthesis: $w_0 = 7$, $d_s = 7.7$ nm; NPs purified with MeOH; reaction: buffered).

This increase in selectivity to ammonium with conversion was also observed for the 7.7 nm NPs, although in a lower extent. This change in behaviour could be related to the reduction of NPs in the reaction medium, as discussed from XPS characterization.

Some works in literature described a lower generation of ammonium in the reduction of nitrite by large Pd NPs due to the lower prevalence of low coordination sites such as edges, corners and defects, where the formation of ammonium is supposed to take place [33]. In this sense, Danmeng Shuai et al. [35] observed an increase in the selectivity to ammonium with decreasing size of Pd NPs supported on carbon nanofibers. The results in the current work are in agreement with the literature, but extremely low selectivities to ammonium were observed in our case. This behaviour is related to the interaction between Pd NPs and AOT, since the aforementioned works were carried out with clean surface NPs. To go deeper on this issue, the selectivity results for the nitrite reduction runs carried out with NPs purified with different solvents, i.e. different degree of removal of AOT, can be considered (Fig. 9). Exceptional selectivity to N_2 can be observed for those samples purified with THF, which can be interpreted in terms of a lower removal of AOT and higher coverage of the Pd NPs, including low coordination sites. Thus NPs purified with THF are less active and exhibit lower selectivity to ammonium. On the contrary, for those NPs purified with a TFE + MeOH mixture a higher removal of AOT is achieved and higher selectivity to ammonium is observed, which is particularly clear in the case of the NPs washed twice. Interestingly, the NPs

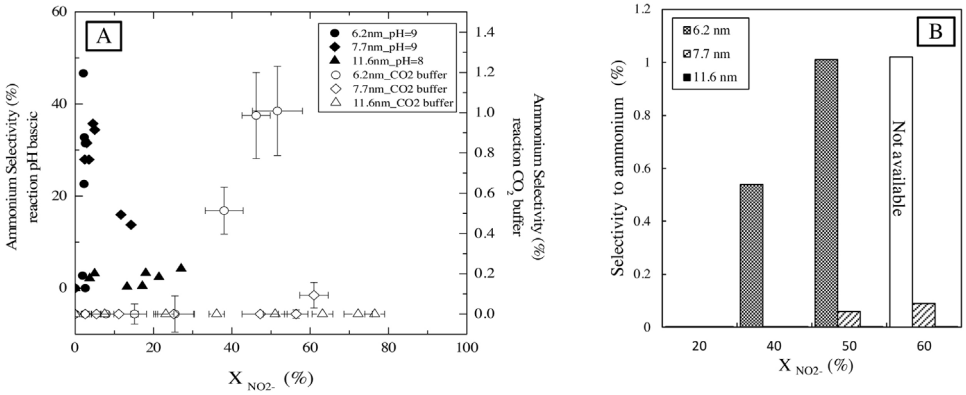

Fig. 8. A: Influence of Pd NPs size and pH of the reaction medium on selectivity to ammonium ion. B: Selectivity to ammonium for buffered medium at constant conversion. (reaction: 2.45 mgPd/L, NPs purified with MeOH).

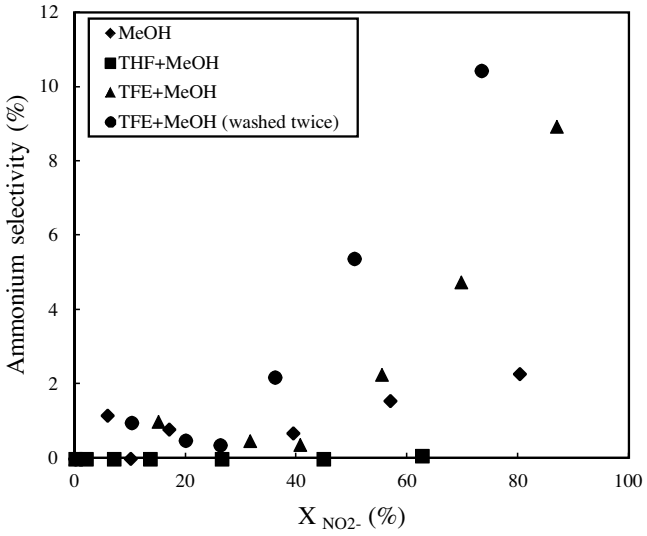

Fig. 9. Selectivity to ammonium in nitrite reduction runs for Pd NPs purified with different solvents (synthesis: $w_0 = 7$, 7.7 nm; reaction: buffered medium, 7.7 mg Pd/L).

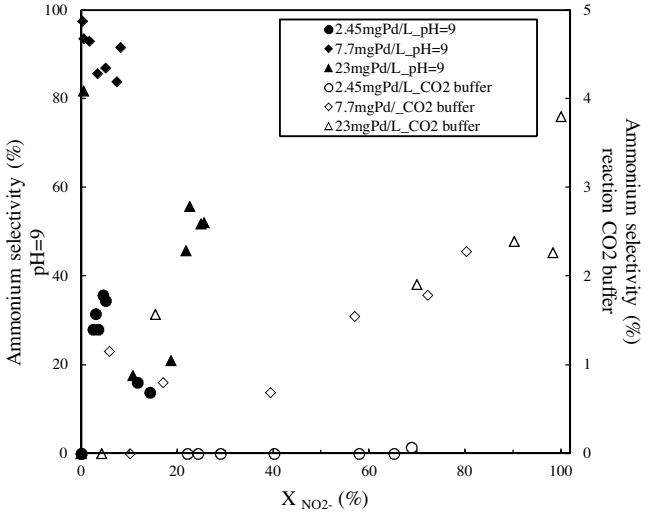

Fig. 10. Influence of ammonium selectivity using different Pd NPs concentration (synthesis: $w_0 = 7$, 7.7 nm; NPs purified with MeOH).

Table 3
Kinetic parameters for nitrite reduction at different Pd concentration (synthesis: $w_0 = 7$, ds = 7.7 nm, reaction: buffered; NPs purified with MeOH).

[Pd] mg Pd/L	$k_{nitrite} \cdot 10^{-3}$ (min^{-1})	R^2	a (mmol/g Pd·min)	TOF (min^{-1})
0.5	0.2	0.868	0.433	0.322
1.5	6	0.992	4.708	3.431
2.45	7	0.995	3.279	2.389
3.3	6	0.995	1.914	1.132
7.7	7	0.997	0.989	0.719
10	20	0.992	2.203	1.603
16.3	27	0.996	1.802	1.314
23	28	0.989	1.179	0.964

washed three times with TFE + MeOH exhibited a lower selectivity to ammonium than these twice-washed ones. It should be noted that after the third wash with the TFE + MeOH mixture, 19% of the Pd NPs were lost in the supernatant and were not available for the reaction. The fraction removed is expected to be integrated by the smallest and better purified NPs.

Regarding selectivity for the reactions carried out at different metal concentrations (Fig. 10), very high selectivity to ammonium was obtained in non-buffered reactions. In buffered reactions ammonium selectivity remained at very low values, but an increase was observed when the metal concentration was increased. At any nitrite conversion, the selectivity values were an order of magnitude higher for the runs carried out with a Pd NPs concentration of 7.7 mg/L. For instance, at 70% nitrite conversion the interpolated values of ammoniums selectivity were 0.1%, 1.6% and 1.9% for the runs carried out with metal concentrations of 2.45, 7.7 and 23 mg/L, respectively. This observation would be consistent with a higher presence of highly active low-coordination sites availabe for the reaction at higher metal concentration, but also indicate that influence of the control regime.

4. Conclusions

The catalytic reduction of nitrite with Pd NPs synthesized by microemulsion using the water-AOT-isooctane system exhibits apparent structure sensitiveness. A lower reaction rate and TOF were observed for small NPs, which can be ascribed to surface blockage caused by strong AOT interaction with low-coordination sites and electron-deficient species on the surface of the Pd NPs. In addition to a decrease of activity, extremely low selectivity to ammonium was achieved, probably due to preferential blockage of the sites responsible for ammonium generation. It must be also considered that different sequences for purification of the NPs lead to different relationship between activity and selectivity. Therefore, the results show the feasibility of reaction control by means of selective blockage of active sites involved in non-desired side reactions.

Appendix A. Supplementary data

Supplementary data associated with this article can be found, in the online version, at http://dx.doi.org/10.1016/j.apcata.2016.10.013.

References

[1] J. Hagen, Industrial Catalysis: A Practical Approach, John Wiley & Sons, 2006.
[2] Z. Niu, Y. Li, Chem. Mater. 26 (2013) 72.
[3] Juan J. Bravo-Suárez, Raghunath V. Chaudhari, Bala Subramaniam, in: Juan J. Bravo-Suárez, Michelle K. Kidder, Viviane Schwartz (Eds.), Novel Materials for Catalysis and Fuels Processing, American Chemical Society, Washington, 2013, p. 3 (Copyright 2013).
[4] P. Mäki-Arvela, D.Y. Murzin, Appl. Catal. A Gen. 451 (2013) 251.
[5] D.Y. Murzin, Catal. Sci. Technol. 1 (2011) 380.
[6] J.P. Rao, K.E. Geckeler, Prog. Polym. Sci. 36 (2011) 887.
[7] S. Ordóñez, E. Díaz, R.F. Bueres, E. Asedegbega-Nieto, H. Sastre, J. Catal. 272 (2010) 158.
[8] N. Toshima, H. Yan, Y. Shiraishi, in: B.C.S. Toshima (Ed.), Metal Nanoclusters in Catalysis and Materials Science, Elsevier, Amsterdam, 2008, p. 49.
[9] L. Hyunjoo, in: J.Y. Park (Ed.), Current Trends of Surface Science and Catalysis, Springer, New York, 2014, pp. 21–43.
[10] J.A. Lopez-Sanchez, N. Dimitratos, C. Hammond, G.L. Brett, L. Kesavan, S. White, P. Miedziak, R. Tiruvalam, R.L. Jenkins, A.F. Carley, Nat. Chem. 3 (2011) 551.
[11] D. Li, C. Wang, D. Tripkovic, S. Sun, N.M. Markovic, V.R. Stamenkovic, ACS Catal. 2 (2012) 1358.
[12] E. Schmidt, W. Kleist, F. Krumeich, T. Mallat, A. Baiker, C Chem. Eur. J 16 (2010) 2181.
[13] E. Sadeghmoghaddam, K. Gaïeb, Y. Shon, Appl. Catal. A Gen. 405 (2011) 137.
[14] Y. Yuan, N. Yan, P.J. Dyson, ACS Catal. 2 (2012) 1057.
[15] I.M. Vilella, I. Borbáth, J.L. Margitfalvi, K. Lázár, S.R. de Miguel, O.A. Scelza, Appl. Catal. A Gen. 326 (2007) 37.
[16] R. Ganguly, N. Choudhury, J. Colloid Interface Sci. 372 (2012) 45.
[17] H. Sato, T. Ohtsu, I. Komasawa, J. Chem. Eng. Jpn. 35 (2002) 255.
[18] L.F. Xiong, T. He, Chem. Mat. 18 (2006) 2211.
[19] W. Zhang, X. Qiao, J. Chen, Mater. Sci. Eng. B 142 (2007) 1.
[20] N. Krishnankutty, M.A. Vannice, J. Catal. 155 (1995) 312.
[21] http://srdata.nist.gov/xps/.

[22] J.A. Baeza, L. Calvo, M.A. Gilarranz, A.F. Mohedano, J.A. Casas, J.J. Rodriguez, J. Catal. 293 (2012) 85.
[23] Y. Zhao, J.A. Baeza, N. Koteswara Rao, L. Calvo, M.A. Gilarranz, Y.D. Li, L. Lefferts, J. Catal. 318 (2014) 162.
[24] V. Höller, K. Rådevik, I. Yuranov, L. Kiwi-Minsker, A. Renken, Appl. Catal. B Environ. 32 (2001) 143.
[25] A.M. Perez-Coronado, L. Calvo, N. Alonso-Morales, F. Heras, J.J. Rodriguez, M.A. Gilarranz, Colloids Surf. A 497 (2016) 28–34.
[26] I. Mikami, Y. Sakamoto, Y. Yoshinaga, T. Okuhara, Appl. Catal. B Environ. 44 (2003) 79.
[27] N. Semagina, A. Renken, D. Laub, L. Kiwi-Minsker, J. Catal 246 (2007) 308.
[28] F. Chen, Z. Zhong, X.J. Xu, J. Luo, J. Mater. Sci. 40 (2005) 1517.
[29] H. Qian, Z. Zhao, J.C. Velazquez, L.A. Pretzer, K.N. Heck, M.S. Wong, Nanoscale 6 (2014) 358.
[30] U. Prüsse, K. Vorlop, J. Mol. Catal. A Chem. 173 (2001) 313.
[31] W. Lin, W.J. Rieter, K.M.L. Taylor, Angew. Chem. Int. Ed. 48 (2009) 650.
[32] O.S.G.P. Soares, M.F.R. Pereira, J.J.M. Órfão, J.L. Faria, C.G. Silva, Chem. Eng. J. 251 (2014) 123.
[33] J.K. Chinthaginjala, A. Villa, D.S. Su, B.L. Mojet, L. Lefferts, Catal. Today 183 (2012) 119.
[34] J.K. Chinthaginjala, L. Lefferts, Appl. Catal. B Environ. 101 (2010) 144.
[35] D. Shuai, J.K. Choe, J.R. Shapley, C.J. Werth, Environ. Sci. Technol. 46 (2012) 2847.